COMPARISON OF METEOROLOGICAL CONDITIONS DURING MAY AND AUGUST 2010 FLOODS IN CENTRAL EUROPE

MAREK KAŠPAR[1], MILOSLAV MÜLLER[1,2], JOZEF PECHO[3,4]

[1] Institute of Atmospheric Physics AS CR
[2] Charles University, Faculty of Science
[3] Technical University of Liberec
[4] Comenius University, Faculty of Mathematics, Physics and Informatics

Abstract

We compared May and August 2010 precipitation events that produced catastrophic flooding. In May, large rivers (Vistula, Oder) were affected, while smaller rivers (e.g. Lausitzer Neisse) were affected in August. Similarities in precipitation characteristics (duration of several days, daily total maximum of approximately 180 mm) can be explained by similarities in the meso-a scale (thermo-dynamic indicia connected with a cyclonic system of Mediterranean origin). These indicia were more significant in May (extreme and deep vertical wind speed, extreme northerly flux of moisture) than in August (strong but non-extreme northerly flux of moisture) when conditional instability was additionally detected. Obviously more intensive orographic enhancement in the first case and the strong effect of convection in the latter case produced differences in the return periods of precipitation totals (longer return periods in August). Subsequently, the hydrological response was rapid and particularly strong in smaller streams in August.

Keywords: flood, heavy precipitation, meteorological anomaly, return period, orographic precipitation enhancement

1. Introduction

In 2010, several significant flooding events occurred worldwide. From a global viewpoint, the most catastrophic one affected Pakistan in summer (Gaurav et al. 2011), causing 1760 deaths and 9.5 billion U.S. dollars in damage (MunichRe 2012). In Central Europe, summer flooding can also be very devastating, as it was, for example, in July 1997 and in August 2002 (Řezáčová et al. 2005). In 2010, the region experienced several catastrophic floods during the warmer half-year. The events were studied in detail in the affected countries by meteorological and hydrological authorities in the Czech Republic, Germany, Poland, and Slovakia. Cyclones moving along the Vb pathway (van Bebber 1891) were blamed for hundreds of millimeters of precipitation during several days both in May and in August. On the other hand, the events differed from each other not only in terms of the affected catchments but also the course of flooding. The aim of this paper is to elucidate the hydrological differences between the events with respect to meteorological causes and precipitation distribution. The structure of the paper is as follows: (1) a brief description of the events, (2) specification of data and methods, (3) determination of meteorological conditions both before and during the events by means of anomalies in synoptic-scale fields, (4) time/space/intensity analysis of precipitation, (5) conclusions and discussion of the results.

Flooding occurred in the eastern part of Central Europe in the second half of May 2010. The antecedent saturation of the region was high due to rains that occurred at the beginning of the month (Daňhelka and Šercl 2011). Extra-heavy rains that reached their maximum on 16 May were associated with a cyclone passing from the Mediterranean northeastward, becoming almost stationary over Ukraine for several days (Bissolli et al. 2011). The highest precipitation totals were recorded in the western sector of the cyclone at the state border between the Czech Republic, Slovakia, and Poland. This headwater area of the rivers Odra and Vistula is prone to flooding in summer (Čekal, Hladný 2008) due to (i) frequent Mediterranean cyclones trajectories and (ii) a specific configuration of mountain ranges supporting low-level convergence and uplifts of air (Kyselý and Picek 2007). Subsequently, the water stages were even higher than those during the catastrophic flood in July 1997 in some regions, mainly in the upper reaches of the Vistula River in Poland (Bissolli et al. 2011). In the Czech Republic, peak flows reached return periods of more than 50 years at some gauges (Figure 1). Moreover, because heavy precipitation fell over the Flysch Outer Western Carpathians, which are susceptible to landslides, it also had geomorphologic impacts. More than 150 mostly small landslides originated only in the eastern part of the Czech Republic, including a kilometer-long rockslide along the southern slope of Mt. Girová, the Beskydy Mts. (Pánek et al. 2011).

During the first decade of August 2010, flooding occurred in many rivers over the western part of the Czech Republic, with high return periods concentrated in a rather small region at the state border between the Czech Republic, Germany and Poland (Figure 1). Heavy rains reaching their maximum on 7 August were more concentrated in time than they were in May. They were associated with a rather shallow cyclone passing from the Mediterranean to the north. The most affected river basins were Lausitzer Neisse (a left-sided tributary of Oder) and the neighboring

To be quoted as:
Kašpar, M. – Müller, M. – Pecho, J. (2013): Comparison of meteorological conditions during May and August 2010 floods in Central Europe
AUC Geographica, 48, No. 2, pp. 27–34

right-sided tributaries of Elbe (Müller and Walther 2011). The water levels were the highest ever recorded at some smaller streams. Moreover, the flood caused the Niedów Dam on the river Witka to break.

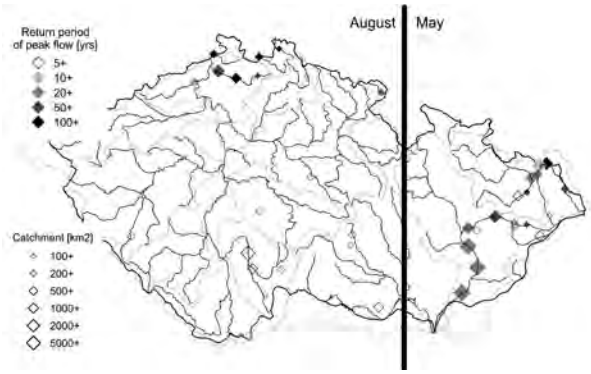

Fig. 1 Return periods of peak flows reached in May 2010 and in August 2010 in the Czech Republic (the right and the left part of the figure, respectively). The size of the sign represents the area of the catchment in km^2.

2. Data and methods

2.1 Meteorological data and their processing

Müller et al. (2009) demonstrate that heavy rains, which produce floods in major rivers in the Czech Republic, are regularly associated with the appearance of climatologically high or low values of certain thermo-dynamic variables in specific meso-*a* scale areas in Europe and the Northern Atlantic. Subsequent studies (e.g., Kašpar and Müller 2009; Müller and Kašpar 2010) come to similar conclusions within the broader region of Central Europe and indicate that such thermo-dynamic anomalies may be an effective indicator of causal synoptic processes. Based on these findings, we opted for a more in-depth analysis of the events using the method presented below.

We used the 6-hourly NCEP/NCAR Reanalysis data set (Kalnay et al. 1996) covering the area of interest, 0°–40° E by 40°–60° N, with a horizontal resolution of 2.5°. We limited ourselves to the 60-year period spanning from 1951 to 2010. We considered the values of basic variables directly offered by the data set at the following isobaric levels: 1000, 925, 850, 700, 600, 500, 400, and 300 hPa. These variables include air temperature, geopotential height, specific and relative humidity, zonal and meridional wind components, and vertical velocity. In addition to the basic variables, we calculated several variables derived from gradients, divergences, vorticities, fluxes, and Lagrangian tendencies.

We standardized the sample distributions of the values of all variables in each grid point and on each calendar day to reduce the effect of the climatological annual cycle. Moreover, we standardized the time series individually at 00, 06, 12 and 18 UTC to reduce the possible effects of a diurnal cycle. We used a standardization procedure that eliminates the skewness and kurtosis in these distributions and set their mean to 0 and their standard deviation to 1. In the majority of cases, this is an adequate standardization procedure and yields the "near normality" of the resulting distributions (e.g., Jobson 1991).

First, we eliminated the skewness by a unified extension of the Box-Cox transformation proposed by Yeo and Johnson (2000). The extension is a non-linear power transformation defined as

$$\begin{aligned}
&Y(x) = [(x+1)^{\tilde{\alpha}} - 1]/\,\tilde{\alpha},\ x \geq 0 \text{ and } \tilde{\alpha} \neq 0;\\
&Y(x) = 1n\,(x+1),\ x \geq 0 \text{ and } \tilde{\alpha} = 0;\\
&Y(x) = -[(-x+1)^{2-\tilde{\alpha}} - 1]/(2-\tilde{\alpha}),\ x < 0 \text{ and } \tilde{\alpha} \neq 2;\\
&Y(x) = -1n\,(-x+1),\ x < 0 \text{ and } \tilde{\alpha} = 2. \qquad (1)
\end{aligned}$$

In Eq. (1), $Y(x)$ is the transformed value of an original value x and is the time-smoothed transformation parameter corresponding to a given calendar day. We estimated the parameter for each calendar day by minimizing the skewness of the sample-transformed distribution of $Y(x)$. To smooth the parameter in time, we applied a 1-D Gaussian filter to the time series of the estimations of this parameter. For accuracy, we did not consider 29 February. For leap years, we used the corresponding to 28 February. On calendar days with the index j, the time-smoothed parameters were calculated by

$$\alpha_j = \frac{\sum_{jj=j-k}^{j+k} \alpha_{jj} G(jj, j)}{2k+1}, \qquad (2)$$

where a_{jj} is the estimation of the parameter on the calendar day with the index jj and the discrete Gaussian function $G(jj,j)$ is given by

$$G(jj, j) = \frac{1}{\sqrt{2\pi}s} e^{-\frac{(jj-j)^2}{2s^2}}. \qquad (3)$$

After some testing, we subjectively selected Gaussian smoothing with a standard deviation $s = 30$ days and time window $k = 3s = 90$ days. The smoothing of the parameter is sufficient to significantly reduce the effect of outliers and to eliminate the high-frequency time oscillations over periods of less than roughly three months. On the other hand, the smoothing is reasonably strong in eliminating the annual cycle of the skewness of transformed distributions, which thus oscillates around zero.

Next, we removed the kurtosis by the modified Box-Cox transformation introduced for symmetric distributions by John and Draper (1980):

$$\begin{aligned}
&Z(y) = \text{SIGN}\,[(|y - y_M| + 1)^{\tilde{\beta}} - 1]/\,\tilde{\beta},\ \tilde{\beta} \neq 0;\\
&Z(y) = \text{SIGN}\,[1n(|y - y_M| + 1)],\ \tilde{\beta} = 0. \qquad (4)
\end{aligned}$$

In Eq. (4), $Z(y)$ is the transformed value of a value $y = Y(x)$ obtained by Eq. (1), y_M is the median of a given sample distribution of y, SIGN is the sign of the original value before taking absolute values and $\tilde{\beta}$ is the time-smoothed transformation parameter corresponding to a given calendar day. We estimated the parameter for each calendar day by minimizing the kurtosis of the sample-transformed distribution of $Z(y)$. To smooth the parameter in

time, we applied the 1-D Gaussian filter described by Eqs. (2) and (3) with standard deviation s = 30 days and time window $k = 3s$ = 90 days.

Finally, we set the mean to 0 and the standard deviation to 1 by the application of the standard score

$$\hat{z} = \frac{z - \tilde{\mu}}{\tilde{\sigma}}, \tag{5}$$

where $\hat{z}$ is the standardized value of a value $z = Z(y)$ obtained by Eq. (4), $\tilde{\mu}$ is the time-smoothed mean and $\tilde{\sigma}$ is the time-smoothed standard deviation of the sample-transformed distribution of $Z(y)$ corresponding to a given calendar day. To smooth the parameters in time, we applied the 1-D Gaussian filter described by Eqs (2) and (3) with standard deviation s = 10 days and time window $k = 3s$ = 30 days.

Because heavy rains in May and August 2010 were clearly conditioned by atmospheric processes occurring on a time scale longer than 6 hours, we additionally considered the daily means of the standardized variables using the formula

$$\hat{z}_d = \frac{0.5\hat{z}_{06}^{d} + \hat{z}_{12}^{d} + \hat{z}_{18}^{d} + \hat{z}_{00}^{d+1} + 0.5\hat{z}_{06}^{d+1}}{4}, \tag{6}$$

where the values of $\hat{z}$ at 06, 12 and 18 UTC on the day d and at 00 and 06 UTC on the following day $d + 1$ are included. We defined the daily period from 06 UTC to 06 UTC on the following day to ensure the agreement with the period during which daily precipitation totals were measured.

In the last step, we assessed the probability of not exceeding high and low values of each standardized variable at each grid point. We applied the three-parametric generalized extreme value (GEV) distribution (Coles 2001) using a block maxima approach.

Regarding high values, we assembled the quarterly maxima from 1951 to 2010 to ensure the sufficient independency of the sample and explanation of the distribution of 1% of the highest daily means $\hat{z}_d$ and 0.25% of the highest 6-hourly values . Hereinafter, these high values are referred to as $\hat{x}$. Then, we fitted the distribution of the maxima with the GEV distribution. We estimated the GEV parameters by the method using L-moments (Hosking and Wallis 1997). L-moments are the linear combinations of the realizations of a variable and represent a set of scale and shape statistics alternative to conventional (product) moments. The method using L-moments is computationally simpler and may give better estimations of the parameters for moderate sample sizes than the maximum likelihood method and the methods of conventional moments (Hosking et al. 1985).

The probability of not exceeding p of a value $\hat{x}$ is calculated by

$$p(\hat{x}) = \left[F(\hat{x})\right]^{4/(365.2425n)}, \tag{7}$$

where F denotes the cumulative distribution function of the GEV estimated from quarterly maxima and n = 1 for daily means and n = 4 for 6-hourly dataset. Equation (7) presumes the independence of the dataset, which does not have to be fulfilled each time. Nevertheless, this can be neglected because of our purposes focused on the comparison of the events. Finally, the corresponding return period N in units of year can be estimated for the most extreme values $\hat{x}$ of as

$$N(\hat{x}) = \frac{1}{4\left(1 - F(\hat{x})\right)}. \tag{8}$$

Regarding low values, we employed the same procedure, but we used the re-analysis dataset multiplied by –1 as an input. The actual probability of not exceeding these values is then equal 1 – p. We defined the positive and negative anomalies in a given variable as a contiguous space which is characterized by the probability of not exceeding the values of the variable equal to or greater than 0.99 (0.9975 for 6-hourly dataset) and equal to or less than 0.01 (0.0025 for 6-hourly dataset), respectively.

2.2 Precipitation data and their processing

We searched the daily precipitation totals of the entire territory of the Czech Republic (measured by the Czech Hydrometeorological Institute) and, in part, those of neighboring countries as well: Slovakia (by the Slovak Hydrometeorological Institute), Poland (by the Institute of Meteorology and Water Management), and Germany (by the German Weather Service). Apart from daily totals, we also searched two- and three-day precipitation totals.

To express the extremeness of precipitation totals at individual gauge stations within the Czech Republic, we determined the return periods of precipitation totals at more than 700 gauges. To this end, we again applied the three-parametric GEV distribution that was found to represent a suitable model for precipitation extremes in most regions of the Czech Republic (Kyselý and Picek 2007). We used the parameters of the GEV distribution estimated by means of the L-moment algorithm (Hosking and Wallis 1997) and the region-of-influence (ROI) method (Burn 1990; Gaál and Kyselý 2009). In contrast to local (at-site) frequency modeling, in which inference is drawn solely based on data observed at individual gauges, the ROI method makes use of regions, in which all regional data, weighted by a dissimilarity measure, are used to estimate the parameters of the distribution of extremes at a given gauge station. The advantage of the ROI method compared to the local analysis is that sampling variations in the estimates of model parameters and high quantiles may be substantially reduced, and the inference becomes more robust (for more details see Kyselý et al. 2011).

3. Analysis of thermo-dynamic anomalies

We performed the objective detection of positive and negative anomalies in thermodynamic variables

just before and during heavy rainfall episodes in May and August 2010. We focused on significant anomalies and their spatial extent in light of the probability of not exceeding high and low values at individual grid points. The anomalies, which can be interpreted in terms of synoptic-dynamic meteorology and illustrate both similar and different attributes among the episodes, are discussed in the following sub-sections.

3.1 May 2010 event

The development of the upper-level and lower-level thermo-baric fields just before and during the event is illustrated in Figure XIII (colour appendix). An omega block over the eastern North Atlantic and Western Europe preceded the onset of the causal cyclonic system. The block, which was distinguishable particularly at lower levels, enabled the formation of an upper-level cut-off low in the southern portion of a long-wave trough over Western Europe. The center of the low first appeared over the Balearic Islands at approximately 18 UTC on 14 May. At the same time, strong cyclogenesis initiated near the surface on the front (eastern) side of the low. Figure XIIIa indicates that cyclogenesis took place according to the classic Petterssen scheme of a type B development (Petterssen and Smebye 1971) as the upper-level low spread over a pre-existing lower-level baroclinic area. The strength of the cyclogenetic processes is characterized by intense cyclonic vorticity advection at upper levels ahead of the low in Figure 2. In accordance with the quasigeostrophic approach, apparent vertically increasing vorticity advection ahead of the low triggered synoptic-scale ascending motions, leading to the increase and extension of cyclonic vorticity downward and downstream in a sloped zone. The completion of vertical coupling between the lower-level baroclinic area and the upper vorticity maximum led to the development of a vertically deep and thermally asymmetric cyclone.

While the cyclone propagated to the north-east across the Adriatic Sea and over eastern Romania (Figure XIIIb,c,d), it intensified partially due to lee effects south of the Alps and Carpathian Mountains (Bissolli et al. 2011). Such a cyclone pathway, which transports subtropical air of significant water vapor content northward, is well known for its role in bringing persistent and heavy rainfall to Central Europe (e.g., Mudelsee et al. 2004). However, the specific cyclone pathway is clearly only one of many ingredients important for producing extreme precipitation. Figures 3, 4, and 5 reveal some other thermo-dynamic indicia that could favor extreme precipitation during the event. One-day-averaged fields are used to stress the importance of the persistence of favorable thermo-dynamic conditions. Figure 3 shows extremely strong and vertically deep lifting on the western flank of the cyclone supporting precipitation throughout the troposphere over a large area of Central Europe. Upward motions at upper levels were linked to a baroclinic zone characterized by the widespread warm advection of moist air from the south and east directions, while upward motions at lower levels occurred in the relatively cold air mass southwest from the strong frontal zone (Figure 4). The upward motions at lower

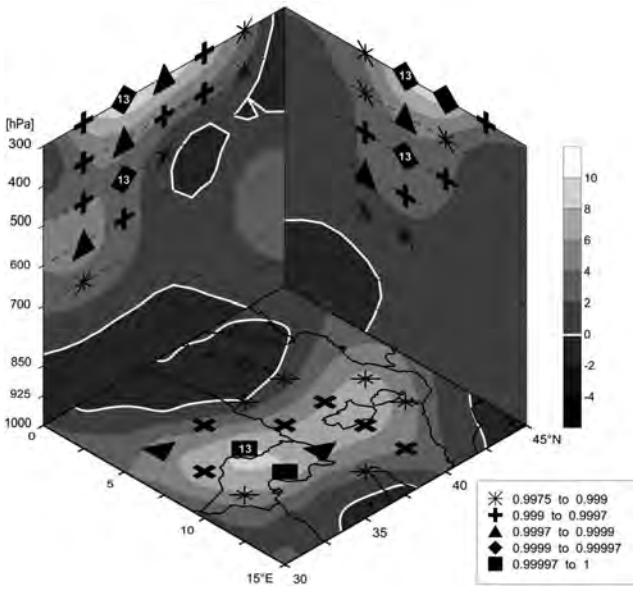

Fig. 2 Three-dimensional projection of the maxima of absolute vorticity advection and maxima of the corresponding probability of not exceeding the values in the selected sub-region on 14 May 2010 at 18 UTC. The values of the advection are depicted by shading in [10^{-9} s^{-2}]. Positive and negative values correspond to cyclonic and anticyclonic vorticity advection, respectively. The probabilities of not exceeding the values are evaluated at grid points in the 850–300 hPa layer and are depicted by symbols according to the legend. Corresponding return periods equal to or greater than 10 years are depicted inside the symbols.

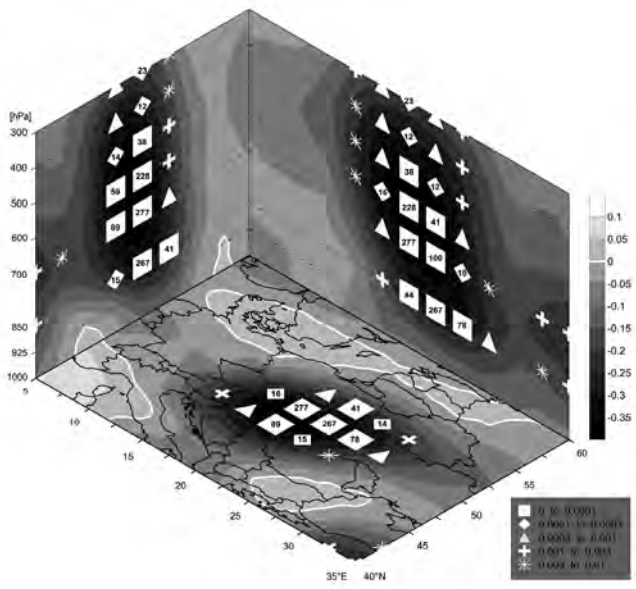

Fig. 3 Same as Figure 2, but for the minimum vertical velocities in the p-system on 16 May 2010. The positive and negative values, in [Pa s^{-1}], correspond to downward and upward motions, respectively.

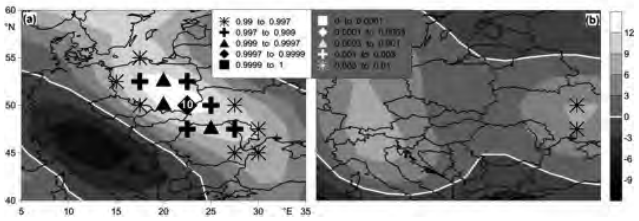

Fig. 4 Southwest to northeast temperature gradient and the corresponding probability of not exceeding the values at (a) 850 and (b) 500 hPa on 16 May 2010. The values of the gradient are depicted by shading in [10^{-6} K m^{-1}]. The positive and negative values correspond to the temperature increase and temperature decrease from the southwest to the northeast, respectively. The probabilities of not exceeding the values are depicted at grid points by symbols according to the legend.

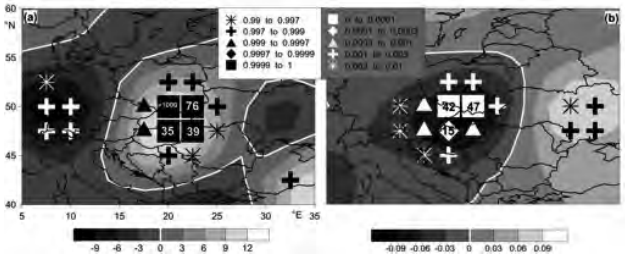

Fig. 5 Selected dynamic variables and the corresponding probability of not exceeding the values at 850 hPa on 16 May 2010. The values of the variables are depicted by shading, and the probabilities of not exceeding the values are depicted at grid points by symbols according to the legend. Corresponding return periods equal to or greater than 10 years are depicted inside the symbols. (a) Flow convergence in [10^{-6} s^{-1}]. The positive and negative values correspond to convergence and divergence, respectively. (b) Meridional flux of moisture in [kg m^{-2} s^{-1}]. The positive and negative values correspond to southerly and northerly moisture flux, respectively.

levels were linked to extremely strong air convergence (Figure 5a) resulting from the confluence to and difluence from the area of enhanced horizontal pressure gradient. Figure 5b shows a strong northerly moisture flux at lower levels, which was linked to strong northerly flow in the area of enhanced horizontal pressure gradient and which supplemented moisture fluxes from the south and east directions at upper levels. Apart from the significant supply of moisture to the area of upward motions, the northerly moisture flux most likely played a role in the orographic enhancement of precipitation on the northern slopes of mountains where additional uplift triggered particularly high rainfall intensities (Section 4).

3.2 August 2010 event

Figure XIV indicates that upper level thermo-baric conditions played a significant role in the development of the causal cyclonic system. The onset of the event was characterized by the deepening of an initially shallow upper level trough with the axis extending from the eastern North Atlantic to the western Mediterranean (Figure XIVa). The spreading of the trough to the southeast over a pre-existing baroclinic area supported lower-level cyclogenesis apparent over northern Italy at 18 UTC on 5 August (Figure XIVb). Figure 6 demonstrates the strength and extent of the cyclogenetic processes on the front side of the through using quasi-geostrophic thinking (see Sect. 3.1). It is evident that intense cyclonic vorticity advection affected only the highest tropospheric levels. Therefore, the significant increase in cyclonic vorticity advection with height was limited to upper and middle levels. As a result, a thermally asymmetric cyclone developed particularly at these levels. The cyclone extended down to the surface layer as well; however, there, the cyclonic circulation was weak (Figure XIVb).

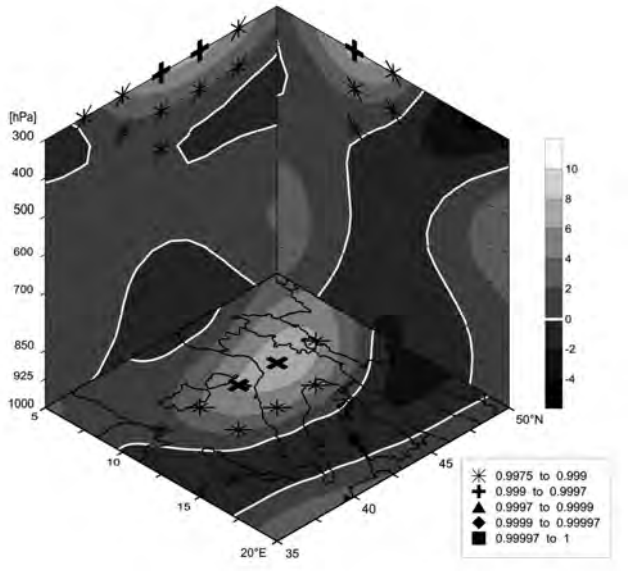

Fig. 6 Same as Figure 2, but for 5 August 2010 at 06 UTC.

While the cyclone slowly moved initially to the east and later to the northeast over the eastern part of central Europe, it weakened (Figure XIVc,d). At the same time, however, the horizontal temperature gradient sharpened between colder air over Western Europe and very warm air over Eastern Europe. Figure 7 reveals a strong and widespread southwest to northeast temperature gradient, which led to the rapid strengthening of baroclinity over Central Europe. In addition, aerological sounding at the central European station Prague-Libuš indicates a vertically deep conditional instability on 7 August 00 UTC, with the values of CAPE and CIN equaling 190 J kg^{-1} and −5 J kg^{-1}, respectively (www.weather.uwyo.edu/upperair). The combination of the synoptic-scale baroclinity and upward motions in the baroclinic zone (Figure 8) with the conditional instability in the sub-synoptic scale could favor the convection of precipitation during an earlier stage of the event.

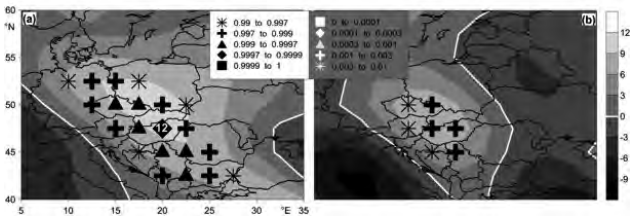

Fig. 7 Same as Figure 4, but for 6 August 2010.

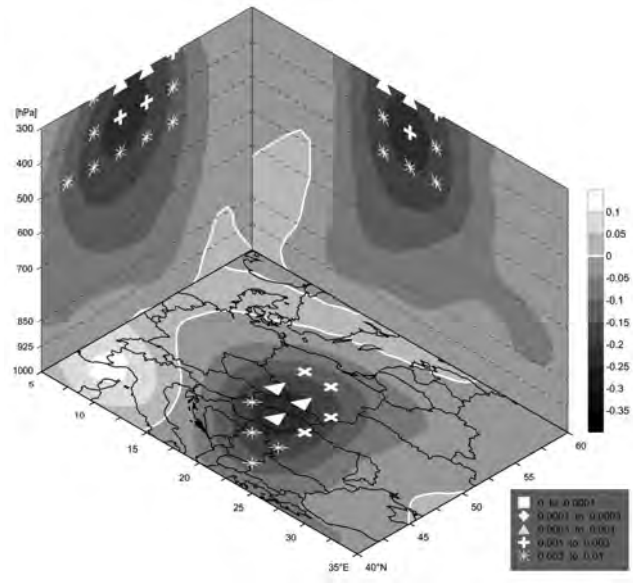

Fig. 8 Same as Figure 3, but for 6 August 2010.

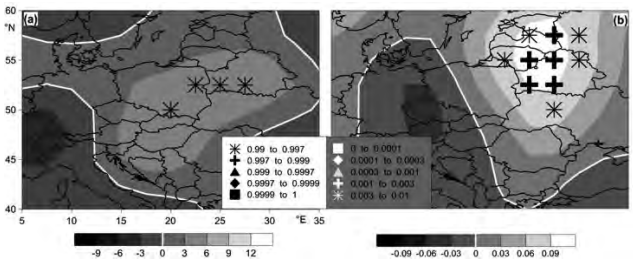

Fig. 9 Same as Figure 5, but for (a) flow convergence on 6 August 2010 and (b) meridional flux of moisture on 7 August 2010.

Figures 8 and 9 complete the description of the extremeness of thermo-dynamic conditions in the meso-a scale. Strong and persistent upward motions occurred only at upper levels (Figure 8), where they were related to well-developed cyclonic circulation. By contrast, non-extreme upward motions connected with strong but rather non-extreme air convergence (Figure 9a) occurred inside the baroclinic zone at lower levels. Due to the weakened horizontal pressure gradient there, the northerly moisture flux to the rainfall area was also non-extreme (Figure 9b). Unlike in the May 2010 event, both extreme and non-extreme (but still favorable) thermo-dynamic indicia can be identified. Therefore, their combined effect was most likely much more crucial in the production of extreme precipitation than the effect of individual ones.

4. Precipitation analysis

The daily precipitation totals observed during the studied events are depicted in Figure XV. From this point of view, the events appear rather similar. Apart from large regions with daily totals of tens of millimeters, there was a limited area with higher precipitation both in May and in August. In May, it was concentrated around the Moravskoslezske Beskydy Mts.; in August, the main affected area was situated around the Jizerske hory Mts. and the Luzicke hory Mts. The highest daily totals were also very similar: 185.2 mm at the Polish gauge Straconka (on 16 May) and 179.0 mm at the Czech gauge Hejnice (on 7 August).

However, there is a substantial difference between the events regarding the return periods of precipitation totals (Figure 10). For example, the daily total of 100 mm had the return period approximately 20 years in May while about 100 years at most gauges in August. It means that in the latter event, precipitation affected a region where heavy rains are significantly less frequent. This fact is even more visible if we compare 3-day totals. In May, they were about twice as high as in August, whereas respective return periods were still longer in August.

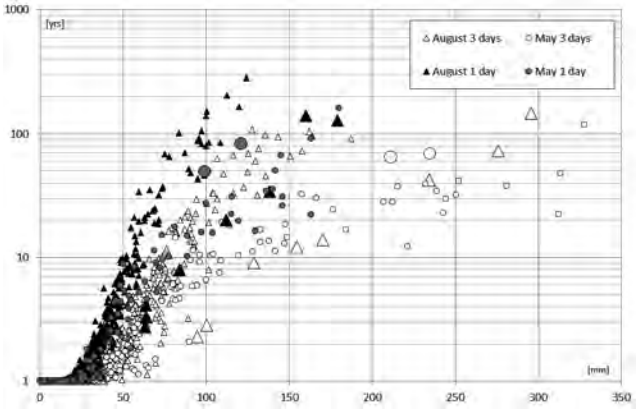

Fig. 10 Maximum one-day and three-day precipitation totals (x-axis) and their return periods (y-axis) at Czech gauge stations during the studied events. Outstanding values discussed in text are marked with big signs.

Nevertheless, several gauges recorded high precipitation totals in August but reached significantly shorter return periods in comparison to other gauges (Figure 10). Three of them even belonged to the highest totals (both daily and 3-day) which were detected in August. In fact, their return periods were similar to those from May! No analogous anomaly occurred in May when only two gauges reached slightly higher return periods than other gauges, despite of similar totals.

Therefore we also studied the relationship between reached precipitation totals and their return periods (if available) on one hand and the position of respective gauges on the other hand (Figure XVI). The above mentioned gauges with high totals but rather short return periods in August were concentrated in the eastern part

of the affected area where the Jizerske hory Mts. and the Giant Mts. constitute a significant barrier for northern winds. Here, as well as in the Moravskoslezske Beskydy Mts. in May, we can recognize a significant role of the orographic enhancement of precipitation. The leeward (~southern) side of the mountains was affected by the precipitation shadow. High precipitation totals occurred not only on the tops of mountains but also both in front of and just behind them. For example, the aforementioned gauges Straconka and Hejnice are situated at an altitude only approximately 400 meters above sea level but still in the vicinity of much higher mountain ranges. On the contrary, the larger (western) part of the area mostly affected by precipitation in August is obviously less orographically exposed.

This result well corresponds with the meteorological conditions described in Section 3. In May, meteorological conditions were characterized by extremely strong thermo-dynamic anomalies. One of these anomalies was a strong moisture flux from the north, which generally supports the orographic enhancement of precipitation along the northern slopes of mountains.

In August, on the contrary, thermo-dynamic anomalies were less significant in the meso-a scale. On the other hand, we can assume a significant role of convection during the latter event because of the detected conditional instability in the area of a strong baroclinic zone.

5. Conclusions

We compared two Central European heavy precipitation events that produced catastrophic flooding in the warm season of 2010. Both precipitation events lasted several days and were characterized by similar maxima of daily totals. These observations can be explained by similarities in meteorological conditions. In both cases, thermo-dynamic indicia in the meso-a scale were detected that are favorable for the production and prolongation of heavy rains. The indicia were connected with a cyclonic system of the Mediterranean origin. The final effects of the indicia were a significant supply of moisture highlighted by strong northerly moisture fluxes into the area of strong upward motions.

Despite these similarities, the events differed from the viewpoint of the hydrological course. While large rivers (Vistula, Oder) also overflowed in May, the August event was limited to smaller streams (Lausitzer Neisse); nevertheless, the peak flows in August can be hardly compared with any other known flood that occurred before. These differences can be explained by dissimilarities in the character and the distribution of precipitation.

In May, heavy rains affected the headwater area of the rivers Oder and Vistula, which is prone to long-lasting, synoptically driven, and orographically enhanced precipitation. Therefore, the return periods of precipitation totals were only approximately 20 years at the majority of gauges, regardless of considering daily or three-day precipitation totals. Indeed, the meteorological conditions were characterized by extremely strong thermo-dynamic anomalies. One of these anomalies was a strong moisture flux from the north, which generally supports the orographic enhancement of precipitation along the northern slopes of mountains.

In August, on the contrary, thermo-dynamic anomalies were less significant in the meso-a scale. Nevertheless, precipitation was also enhanced by orography in part of the most affected area. On the other hand, daily totals of approximately 100 mm were also reached at many gauges with significantly lower orographic effects. We attribute this observation to the effect of convection, which can be assumed because of the detected conditional instability in the area of a strong baroclinic zone. Because the intense precipitation extended to an area with low orographic exposure, the return periods of daily totals in this limited area were much higher than in May. Subsequently, the hydrological response was rapid and particularly strong at smaller streams there.

Acknowledgements

The study was supported by the Czech Science Foundation under the project P209/11/1990. NCEP Reanalysis data were provided by the NOAA/OAR/ESRL PSD, Boulder, Colorado, USA, from their Web site at http://www.esrl.noaa.gov/psd/. We would also like to thank J. Kyselý and L. Gaál from the Institute of Atmospheric Physics in Prague for implementing the Region of Influence method.

REFERENCES

BISSOLLI, P., FRIEDRICH, K., RAPP, J., ZIESE, M. (2011): Flooding in eastern central Europe in May 2010 – reasons, evolution and climatological assessment. Weather 66(6), 147–153. DOI: 10.1002/wea.759

BURN, D. H. (1990): Evaluation of regional flood frequency analysis with a region of influence approach. Water Resources Research 26(10), 2257–2265. DOI: 10.1029/WR026i010p02257

ČEKAL, R., HLADNÝ, J. (2008): Analysis of flood occurrence seasonality on the Czech Republic territory with directional characteristics method. Acta Universitatis Carolinae Geographica 43(1–2), 3–14.

COLES, S. (2001): An introduction to statistical modeling of extreme values. London, Springer Verlag.

DAŇHELKA, J., ŠERCL, P. (2011): Floods in the Czech Republic in 2010. Meteorologické zprávy 64(1), 4–9. [in Czech, with an English abstract]

GAÁL, L., KYSELÝ, J. (2009): Comparison of region-of-influence methods for estimating high quantiles of precipitation in a dense dataset in the Czech Republic. Hydrology and Earth System Sciences 13(11), 2203–2219.

GAURAV, K., SINHA, R., PANDA, P. K. (2011): The Indus flood of 2010 in Pakistan: a perspective analysis using remote

sensing data. Natural Hazards 59(3), 1815–1826. DOI: 10.1007/s11069-011-9869-6

HASTINGS, D. A., DUNBAR, P. K., ELPHINGSTONE, G. M., BOOTZ, M., MURAKAMI, H., MARUYAMA, H., MASAHARU, H., HOLLAND, P., PAYNE, J., BRYANT, N. A., LOGAN, T. L., MULLER, J.-P., SCHREIER, G., MACDONALD, J. S. (1999): The Global Land One-kilometer Base Elevation (GLOBE) Digital Elevation Model, Version 1.0. National Oceanic and Atmospheric Administration, National Geophysical Data Center, 325 Broadway, Boulder, Colorado 80305-3328, U.S.A. Digital data base on the World Wide Web (URL: http://www.ngdc.noaa.gov/mgg/topo/globe.html) and CD-ROMs.

HOSKING, J. R. M., WALLIS, J. R. (1997): Regional frequency analysis: an approach based on L-moments. Cambridge, Cambridge University Press.

HOSKING, J. R. M., WALLIS, J. R., WOOD, E. F. (1985): Estimation of the generalized extreme value distribution by the method of probability-weighted moments. Technometrics 27(3), 251–261. DOI: 10.2307/1269706

JOBSON, J. D. (1991): Applied Multivariate Data Analysis: Regression and experimental design. London, Springer Verlag.

JOHN, J. A., DRAPER, N. R. (1980): An alternative family of transformations. Applied Statistics 29(2), 190–197.

KALNAY, E., KANAMITSU, M., KISTLER, R., COLLINS, W., DEAVEN, D., GANDIN, L., IREDELL, M., SAHA, S., WHITE, G., WOOLLEN, J., ZHU, Y., CHELLIAH, M., EBISUZAKI, W., HIGGINS, W., JANOWIAK, J., MO, K. C., ROPELEWSKI, C., WANG, J., LEETMAA, A., REYNOLDS, R., JENNE, R., JOSEPH, D. (1996): The NCEP/NCAR 40-Year Reanalysis Project. Bulletin of the American Meteorological Society 77(3), 437–471. DOI: 10.1175/1520-0477(1996)077<0437:TNYRP>2.0.CO;2

KAŠPAR, M., MÜLLER, M. (2009): Cyclogenesis in the Mediterranean basin: a diagnosis using synoptic-dynamic anomalies. Nat. Hazards Earth Syst. Sci. 9(3), 957–965.

KYSELÝ, J., GAÁL, L., PICEK, J. (2011): Comparison of regional and at-site approaches to modelling probabilities of heavy precipitation. International Journal of Climatology 31(10), 1457–1472. DOI: 10.1002/joc.2182

KYSELÝ, J., PICEK, J. (2007): Regional growth curves and improved design value estimates of extreme precipitation events in the Czech Republic. Climate Research 33(3), 243–255. DOI: 10.3354/cr033243

MUDELSEE, M., BÖRNGEN, M., TETZLAFF, G., GRÜNEWALD, U. (2004): Extreme floods in central Europe over the past 500 years: Role of cyclone pathway "Zugstrasse Vb". J. Geophys. Res. 109(D23101), 21 pp. DOI: 10.1029/2004JD005034

MÜLLER, M., KAŠPAR, M. (2010): Quantitative aspect in circulation type classifications – an example based on evaluation of moisture flux anomalies. Phys. Chem. Earth 35(9–12), 484–490. DOI: 10.1016/j.pce.2009.09.004

MÜLLER, M., KAŠPAR, M., ŘEZÁČOVÁ, D. SOKOL, Z. (2009): Extremeness of meteorological variables as an indicator of extreme precipitation events. Atmos. Research 92(3), 308–317. DOI: 10.1016/j.atmosres.2009.01.010

MÜLLER, U., WALTHER, P. (2011): The Neisse Flood 2010 – Analysis and Consequences. Wasserwirtschaft 101(11), 10–14. [in German]

MUNICHRE (2011): NatCatSERVICE. Available at www.munichre.com. [Cited 2013-03-01]

PÁNEK, T., BRÁZDIL, R., KLIMEŠ, J., SMOLKOVÁ, V., HRADECKÝ, J., ZAHRADNÍČEK, P. (2011): Rainfall-induced landslide event of May 2010 in the eastern part of the Czech Republic. Landslides 8(4), 507–516. DOI: 10.1007/s10346-011-0268-6

PETTERSSEN, S., SMEBYE, S. J. (1971): On the development of extratropical cyclones. Q. J. R. Meteorol. Soc. 97(414), 457–482. DOI: 10.1002/qj.49709741407

ŘEZÁČOVÁ, D., KAŠPAR, M., MÜLLER, M., SOKOL, Z., KAKOS, V., HANSLIAN, D., PEŠICE, P. (2005): A comparison of flood precipitation episode in August 2002 with historic extreme precipitation events on the Czech territory. Atmos. Res. 77(1–4), 354–366. DOI: 10.1016/j.atmosres.2004.10.008

VAN BEBBER, W. (1891): Die Zugstrassen der barometrischen Minima. Met. Z. 8, 361–366. [In German]

YEO, I.-K., JOHNSON, R. A. (2000): A new family of power transformations to improve normality or symmetry. Biometrika 87(4), 954–959. DOI: 10.1093/biomet/87.4.954

RÉSUMÉ

Srovnání meteorologických podmínek ve střední Evropě během povodní v květnu a srpnu 2010

Článek porovnává některé aspekty dvou případů silných srážek ve střední Evropě v roce 2010, které zde způsobily významné povodně: v květnu především na Visle a Odře a jejich přítocích, v srpnu spíše na menších tocích, jako je Lužická Nisa. Podobnost některých srážkových charakteristik (vícedenní trvání, maximální denní úhrn přibližně 180 mm) může být vysvětlena podobností meteorologických veličin v meso-a měřítku (termodynamické anomálie spojené s cyklonou středomořského původu). Tyto anomálie byly výraznější při květnové události (extrémní vertikální rychlost větru skrz celou troposféru, extrémní tok vlhkosti od severu) než při události srpnové (silný, ne však extrémní tok vlhkosti od severu), kdy byla naopak dodatečně detekována podmíněná instabilita. Zjevně výraznější orografické navýšení srážek v prvním případě a silný podíl konvekce v druhém případě způsobily odlišnosti v dosažených dobách opakování srážkových úhrnů, které byly při srpnové události větší. Následně i hydrologická odezva na menších tocích byla rychlá a silná.

Marek Kašpar
Institute of Atmospheric Physics
Boční II. 1401
141 31 Praha 4
Czech Republic
E-mail: kaspar@ufa.cas.cz